Supplementary Material

Downscaled projections of Caribbean coral bleaching that can inform conservation planning

van Hooidonk et al.

Table of Contents

1. Methods related to the MOM4.1 model run (adapted from Liu et al. 2014 in review)

For the 21st century climate change experiments, MOM4.1 is driven by the surface forcing fields obtained from the CMIP5 dataset (Taylor et al., 2012), including near surface wind speed, surface air temperature, sea level pressure, surface specific humidity, downwelling shortwave and longwave radiation, and precipitation. The CMIP5 (http://cmip-pcmdi.llnl.gov/cmip5) model data can be downloaded from the Earth System Grid Federation portal (http://pcmdi9.llnl.gov/esgf-web-fe/)for the historical and a future emission scenario. The historical runs are forced by observed atmospheric composition changes that include both anthropogenic and natural climate variability. The future (21st century) simulations are obtained from projections for RCP8.5 (Taylor et al., 2012).

18 CMIP5 models are used to derive the surface forcing fields, initial and boundary conditions (see Table S1). These models are selected because they all show a realistic Atlantic meridional overturning circulation (AMOC) strength in the 20th century and contain all surface flux variables needed for the model experiments. If there are multiple ensemble members available for any given model, we only use the first ensemble member in our analysis. Each of the eighteen CMIP5 models is ranked and weighted based on its ability to replicate the observed annual mean sea surface temperature (SST) for the last 30 years of the 20th century (1971-2000), following Liu et al. (2012). The AMOC strength based on the maximum overturning stream function at 30°N is computed for each CMIP5 during 1971-2000. The rationale for this is that the SST in the Caribbean Sea and Gulf of Mexico depends strongly on the AMOC for its effect on the northward advection of warm surface water through the Yucatan Channel (e.g., Schmittner, 2005). The models are ranked and weighted based on the difference between the calculated AMOC strength and the observed value of 18.0 ± 2.5 Sv (Lumpkin and Speer, 2007); the

smaller the difference, the higher the rank (see Table S1).

We first construct the CMIP5 climatology for the 1971-2000 periods under the historical scenario, and then compute the difference between the weighted ensemble of the CMIP5 climatology and the observed surface forcing climatology. This minimizes the biases in the surface forcing fields obtained from the CMIP5 model simulations. The Coordinated Ocean Research Experiments version-2 (CORE2) surface flux product (Large and Yeager, 2009) is used to derive the observed surface forcing climatology. Then, the difference (the bias-correction term) is added to the CMIP5 surface forcing fields for the RCP8.5 scenario for the period of 1900-2098. The initial and boundary conditions for the temperature and salinity are also bias-corrected following the same methodology used for the surface forcing fields. The observed temperature and salinity climatology are obtained from the U.S. Navy Generalized Digital Environmental Model version 3.0 (GDEM3, Carnes, 2009). The difference between the CMIP5 climatology and the observed (GDEM3) temperature and salinity climatology during the period of 1971-2000 is added to the CMIP5 temperature and salinity for the period of 1900 to 2098.

The weight coefficient (Table S1) is applied to the bias-corrected surface forcing fields, initial and boundary conditions of each CMIP5 model (see Table 1) under the historical and RCP8.5 scenarios. Then, their weighted ensemble averages are derived and used to perform the MOM4.1 experiments. The MOM4.1 simulation is initialized and integrated for 106 years using the bias-corrected CMIP5 surface forcing fields and initial conditions under the historical scenario for the period of 1900-2005. Then, the future MOM4.1 simulations are continuously run from 2006 to 2098 using the bias-corrected CMIP5 surface forcing fields for RCP8.5.

2. Figure S1.

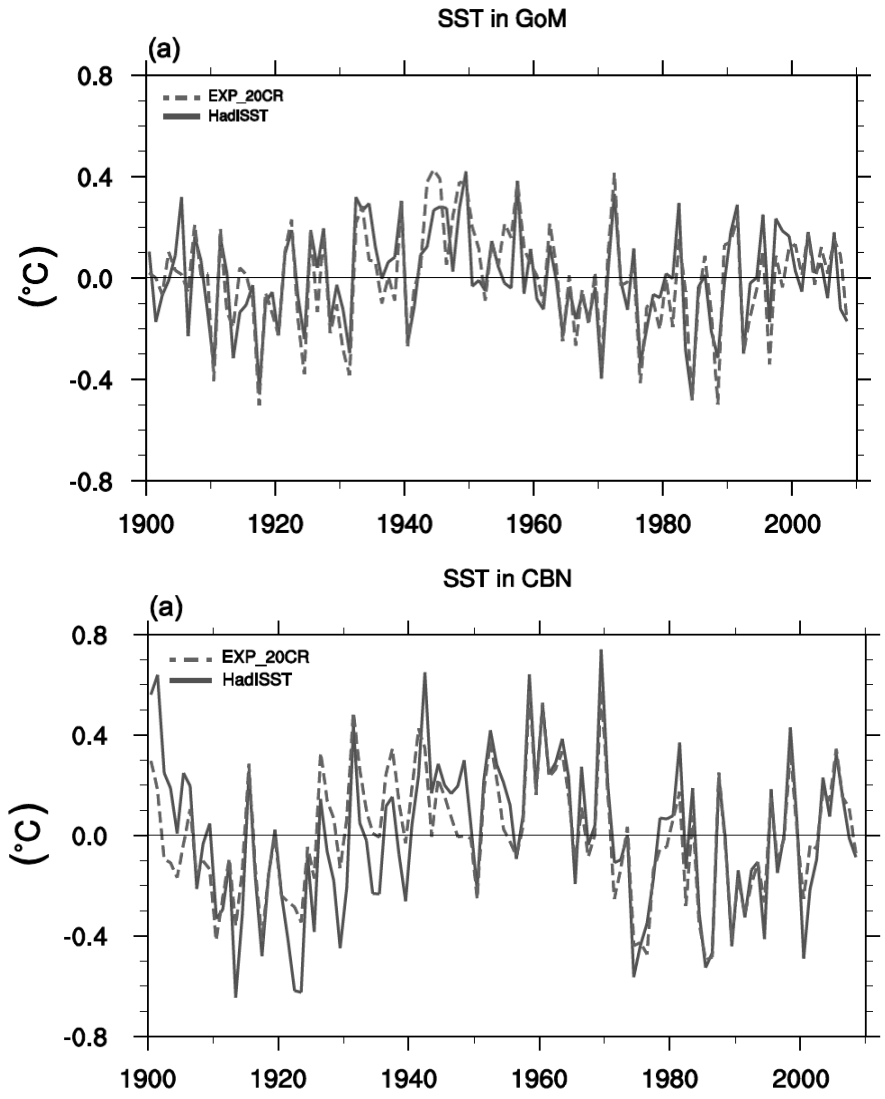

Figure S1. Time series of annual mean SST anomalies averaged over the Gulf of Mexico (top) and Caribbean (bottom) during 1900-2008 obtained from MOM4.1 in hindcast mode and HadISST. For both areas MOM4.1 closely tracks HadISST (figure adapted from Liu et al. 2015).

3. Figure S2.

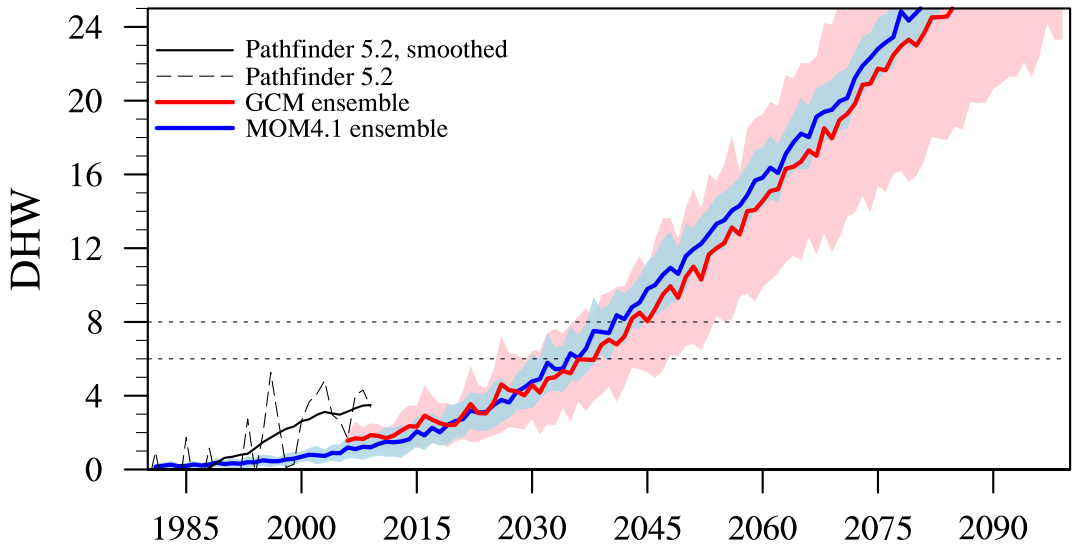

Figure S2. Yearly maximum DHW counts averaged over all reef locations (solid lines) for each year ± 1 standard deviation (shaded area) for all models (GCM ensemble; 2006-2100) and all pseudo-ensemble members (MOM4.1 ensemble, 1982-2100). DHW counts derived from Pathfinder 5.2 for the period 1982-2012 are shown with the dashed line and those data are smoothed with a 10 year running average for comparison with modeled trends. The dotted horizontal lines indicate the annual bleaching (6 DHW) and annual severe bleaching (8 DHW).

4. Figure S3.

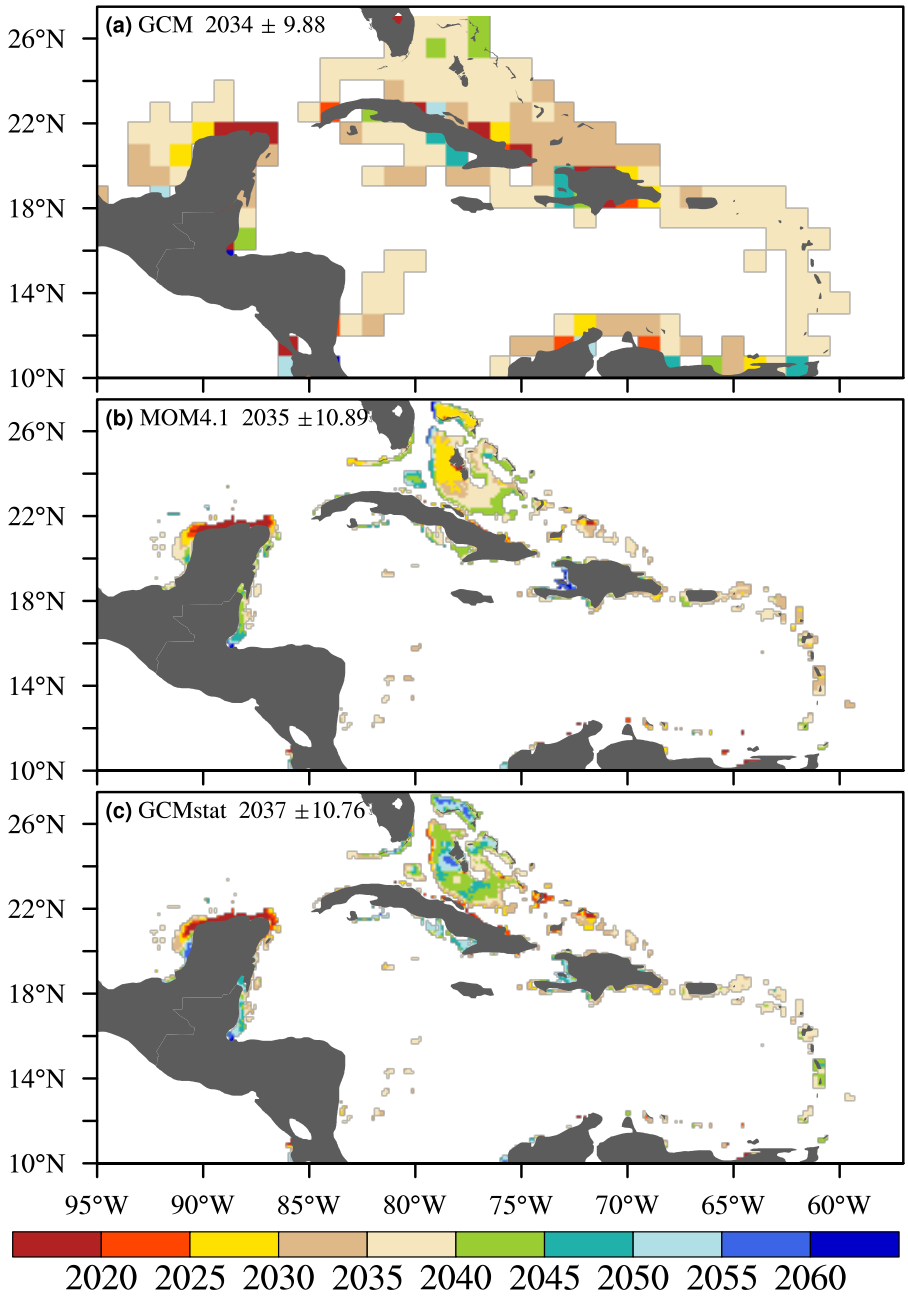

Figure S3. Projected timing in the onset of annual bleaching (>6 DHW) for: (a) the ensemble of Global Climate Models (GCMs, see table S1 for list) at model resolution (1° x 1°), (b) dynamical downscaling through using GCM outputs to force the GFDL Modular Ocean Model (MOM4.1, ~0.1° resolution), and (c) statistically downscaling GCM outputs by replacing the model mean and annual cycle for SST with observed data from 1982-2008 re-gridded to the scale of MOM4.1 (b). For each plot mean year is shown + 1 standard deviation.

5. Figure S4

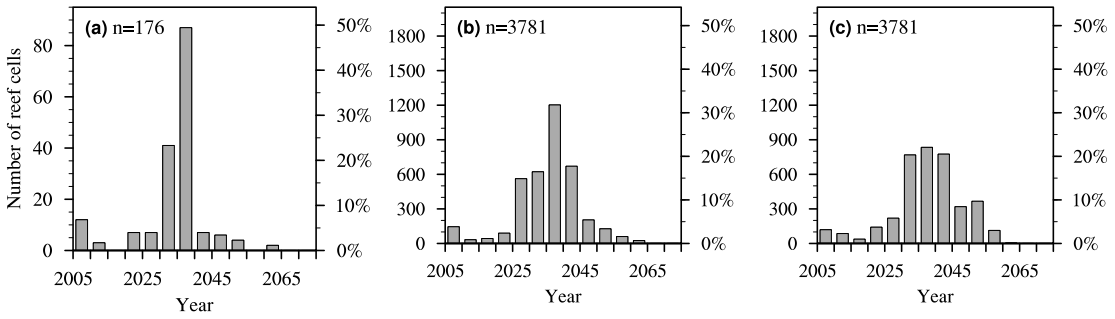

Figure S4. Histograms showing the distribution of the data presented within Fig. S2, values for number and percent of reef locations (grid cells), for (a) the GCM, (b) MOM4, and (c) the statistical downscaling (see Table S4 for data values).

6. Figure S5

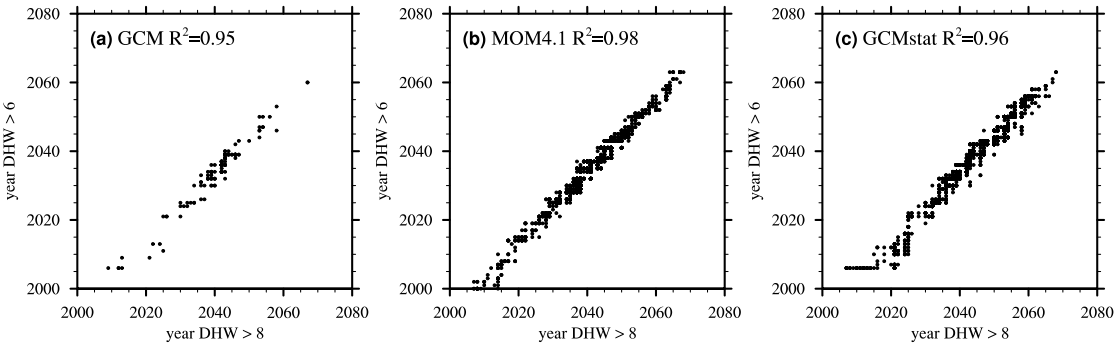

Figure S5. Comparisons of projections of annual bleaching above 6 or 8 DHW for (a) the GCM, (b) MOM4, and (c) the statistical downscaling. On the x-axis the year is plotted when 8 DHW are exceeded annually, on the y-axis when annual conditions exceed 6 DHW.

7. Table S1

Table S1. List of 33 IPCC CMIP5 models used for the ensemble of GCMs (all except grey shade). Models used for the modular ocean model (MOM4.1) are listed first and ranked from highest to lowest based on weightings calculated by comparing modeled to observed AMOC strength values (see methods in section 1.).

Model name	Weighting if used in MOM4
CCSM4	2.38
IPSL-CM5A-LR	2.1
BCC-CSM1.1	1.9
MRI-CGCM3	1.52
IPSL-CM5A-MR	1.48
CSIRO-Mk3.6.0	1.43
GFDL-ESM2G	1.16
GISS-E2-R	1.09
HadGEM2-CC	0.93
GFDL-ESM2M	0.68
HadGEM2-ES	0.65
CanESM2	0.55
MIROC-ESM	0.53
MIROC-ESM-CHEM	0.52
MIROC5	0.36
GFDL-CM3	0.35
CNRM-CM5	0.33
NorESM1-M	0.02
ACCESS1-0	
ACCESS1-3	
BCC-CSM1.1(m)	
CESM1-BGC	

CESM1-CAM5
CESM1-WACCM
CMCC-CESM
CMCC-CM
CMCC-CMS
EC-EARTH
FIO-ESM
HadGEM2-AO
INM-CM4
IPSL-CM5B-LR
MPI-ESM-LR
MPI-ESM-MR
NorESM1-ME

8. Table S2

Table S2**.** Distribution of the projected timing in the onset of annual severe bleaching (>8 DHW) for all three types of projections. Numbers of reef locations (pixels) and percentages are shown. Data correspond to the graphical representation shown in Figure 2 in the paper.

Year Range	GCM (n=176)	%	MOM4.1 (n=3781)	%	GCMstat (n=3781)	%
<2010	7	4	96	3	69	2
2011-2015	4	2	25	1	27	1
2016-2020	0	0	43	1	11	0
2021-2025	3	2	42	1	106	3
2026-2030	4	2	116	3	89	2
2031-2035	10	6	139	4	280	7
2036-2040	27	15	1024	27	600	16
2041-2045	91	52	1173	31	1015	27
2046-2050	16	9	541	14	464	12
2051-2055	9	5	392	10	712	19
2056-2060	3	2	91	2	312	8
2061-2065	0	0	76	2	82	2
>2066	2	1	23	1	14	0

9. Table S3

Table S3**.** Distribution of differences in projected timing of the onset of annual severe bleaching between MOM4.1 (dynamical downscaling) and the GCM ensemble, and between GCM Path (statistical downscaling) and the GCM ensemble. Numbers of reef locations (n=3781) and percentages are shown. Data correspond to the histograms shown in Figure 4 in the paper.

Differences	**MOM4.1-GCM**	**%**	**GCM Path - GCM**	%
> -20	58	1.53	37	0.98
-19 to -15	51	1.35	72	1.90
-14 to -10	164	4.34	107	2.83
-9 to -5	529	13.99	236	6.24
-5 to 0	1095	28.96	631	16.69
1 to 5	816	21.58	1344	35.55
6 to 10	644	17.03	567	15.00
11 to 15	231	6.11	452	11.95
16 to 20	75	1.98	181	4.79
>21	118	3.12	154	4.07

10. Table S4

Table S4. Distribution of the projected timing in the onset of annual bleaching (DHW>6) for all three types of projections. Numbers of reef locations (pixels) and percentages are shown. Data correspond to the histograms shown in Figure S2.

Year Range	GCM (n=176)	%	MOM4.1 (n=3781)	%	GCMstat (n=3781)	%
<2010	12	7	145	4	119	3
2011-2015	3	2	32	1	86	2
2016-2020	0	0	43	1	37	1
2021-2025	7	4	89	2	141	4
2026-2030	7	4	562	15	219	6
2031-2035	41	23	622	16	768	20
2036-2040	87	49	1202	32	834	22
2041-2045	7	4	670	18	775	20
2046-2050	6	3	204	5	319	8
2051-2055	4	2	127	3	366	10
2056-2060	0	0	60	2	113	3
2061-2065	2	1	25	1	4	0
>2066	0	0	0	0	0	0

11. References

Carnes, M. R. (2009), Description and evaluation of GDEM-V 3.0, Tech. Rep. 724/NRL/MR/7300-09-9165, Nav. Res. Lab., Washington, D. C. [Available at http://www7320.nrlssc.navy.mil/pubs/pubs.php.]

Large WG, Yeager SG (2009) The global climatology of an interannually varying air–sea flux data set. *Climate Dynamics*.

Liu, Y, Lee S.-K., Enfield D.B., Muhling B.A., Lamkin J.T., Muller-Karger F. and Roffer M.A., (2015). IPotential Impact of Climate Change on the Intra-Americas Sea: Part-1. A Dynamic Downscaling of the CMIP5 Model Projections. *Journal of Marine Systems*: doi:10.1016/j.jmarsys.2015.01.007

Lumpkin R, Speer K (2007) Global Ocean Meridional Overturning. *Journal of Physical Oceanography*, **37**, 2550–2562.

Schmittner A, Latif M (2005) Model projections of the North Atlantic thermohaline circulation for the 21st century assessed by observations. *Geophysical Research Letters*, **32**, 1–4.

Taylor KE, Stouffer RJ, Meehl GA (2012) An Overview of CMIP5 and the Experiment Design. *Bulletin of the American Meteorological Society*, **93**, 485–498.